J Nanostruct 13(1): 151-158, Winter 2023

RESEARCH PAPER

Green Synthesis of MnO_2 Nanoparticles Using Cumin Extract Composited with Hypericum Plant: Investigation of Antibacterial and Anticancer Properties

*Sareh Ghorbani [1], Younes Mirzaei [1,2], Mohammad Mahdi Bordbar [3] Ali Gholami [2]**

[1] *Ghiaseddin Jamshid Kashani Student Research Institute, kashan, 38576704, Iran*

[2] *Department of Analytical Chemistry, Faculty of Chemistry, University of Kashan, Kashan, 87317-51167, Iran*

[3] *Personal Laboratory, Fasa, 74614, Iran*

ARTICLE INFO

Article History:
Received 11 October 2022
Accepted 26 December 2022
Published 01 January 2023

Keywords:
Antibacterial properties
Anticancer propertie
Cumin extract
Hypercom perforatum
Manganese dioxide nanoparticles

ABSTRACT

Cancer is a major cause of morbidity and mortality. Although there are many treatment techniques, these methods still have many limitations. Nanotechnology is rapidly growing and flourishing in the field of diagnosis and treatment of various diseases. The antibacterial and anticancer properties of nanoparticles (NPs) have made them promising for the treatment of diseases. In this study, manganese dioxide (MnO_2) NPs are green-synthesized by the cumin extract as a regenerator and stabilizer in a co-precipitation method. The synthesized NPs are then composited with the Hypercom perforatum plant. In order to characterize the structure and morphology of MnO_2 NPs, XRD, FTIR, SEM, and TEM analyses are performed. MnO_2 NPs composited with the Hypericum plant were tested for their antibacterial efficacy against strains of Staphylococcus aureus and Pseudomonas aeruginosa. The MTT cytotoxicity assay was used to assess the anticancer effects of MnO_2 NPs composited with the Hypericum plant. In this instance, it was looked into how the NPs affected the human Hela cervical cancer cell line and the cancerous fibroblast cells. Based on these results, MnO_2 NPs can damage Hela cells without damaging healthy cells. This investigation can provide fundamental insights for understanding the antibacterial activity and cytotoxicity of these NPs and point out their applicability for use in the biomedical field.

How to cite this article
Ghorbani S., Mirzaei Y., Bordbar M., Gholami A. Green Synthesis of MnO_2 Nanoparticles Using Cumin Extract Composited with Hypericum Plant: Investigation of Antibacterial and Anticancer Properties. J Nanostruct, 2023; 13(1):151-158. DOI: 10.22052/JNS.2023.01.017

INTRODUCTION

Nanoscience and nanotechnology are significant scientific fields that deal with the use and development of materials made at the nanoscale. Nanoparticles (NPs) with sizes in the range of 1–100 nm can be produced through numerous methods. However, these methods use chemicals that are with a high risk of toxicity and low degradability [1]. Due to their small size and high surface-to-volume ratio, NPs have high effectiveness and durability, being employed in various fields, including biological, physical, chemical, pharmaceutical, and engineering sciences [2].

Although not all bacterial species are pathogenic, dangerous diseases such as cholera, tuberculosis,

* *Corresponding Author Email: agholami@kashanu.ac.ir*

typhus, and anthrax, as well as infections such as blood and urinary infections, wound infections, and many other diseases can be caused by some species of bacteria [3]. Staphylococcus aureus is a gram-positive bacterium and one of the most prominent pathogenic species of staphylococci. Nevertheless, it has become one of the public health concerns due to its intrinsic resistance to antimicrobial agents and drugs [4]. In the last 50 years, Staphylococcus aureus has undergone many genetic changes. This bacterium has a flexible genome, leading to an increase to its pathogenic and drug-resistant strains [5]. Staphylococcus aureus settles in the nose and skin (especially damaged skin), vagina, armpit, and navel of newborn babies [6]. Pseudomonas aeruginosa is a gram-negative bacterium belonging to the Pseudomonadaceae family, having the possibility to survive in a wide range of environments. Pseudomonas aeruginosa is known as an opportunistic pathogen and the most common bacterium associated with hospital infections [7]. This bacterium leads to fatal infections in immunocompromised people such as patients with cancer post-surgery and severe burns or infected with human immunodeficiency virus [8].

Cancer is one of the health problems of today's societies, and many efforts are being made to deal with it. In fact, cancer is complex, inconsistent and heterogeneous, arising from genetic changes. Many factors are responsible for the proper growth and proliferation of normal cells, being appropriate only when the cell proliferation is carefully controlled. In other words, cancer occurs if the regulation of cell proliferation processes is not made correctly, thereby disrupting the normal function and behavior of cells [9, 10]. As the fourth most common cancer in women, cervical cancer accounts for approximately 12% of women's cancers, and is considered the seventh most common cancer in the world. The majority of global cancer cases occur in less developed countries [11].

Hypericum perforatum is a valuable medicinal plant from the Hypericaceae family. Hypercom species are used in different parts of the world such as Europe, America, Africa, and Asia, having astringent, diuretic, analgesic, antidepressant, and disinfection properties. In addition to the aforementioned properties, Hypericum species are used to treat wounds, burns, and bites of poisonous animals in traditional and Chinese medicine. In recent decades, a number of pharmaceutical and phytochemical studies has shown that the antitumor, antidepressant, antibacterial and anti-inflammatory activities of Hypericum species are due to the presence of bioactive compounds, including phloroglucinol, xanthone, and flavonoid derivatives [12].

NPs can cause three types of damage to bacteria: i) they can be located near the bacterial cell and destroy the cell without effectively connecting to its external structure (e.g., the cell wall or cytoplasmic membrane), ii) they can destroy the cell through electrostatic attraction, hydrogen bonding, or van der Waals interaction, and iii) they can penetrate into the cell and directly damage the components inside it (e.g., cytoplasmic proteins or DNA), thus destroying the cell [13]. On the other hand, NPs and drugs can be used with precise targeting to treat cancer cells. This approach is called targeted therapy, being a growing part of treatment for many types of cancer.

Due to its excellent physical and chemical properties, cost-effectiveness, structural diversity and biocompatibility, manganese dioxide (MnO_2) with semiconducting properties has been widely used in various fields of science and technology, including sensors [14], energy storage [15], catalysts [16], bioimaging, and drug release [17, 18]. In general, MnO_2 NPs can act as a multipurpose therapeutic agent to improve tumor therapy [19]. With regard to structural properties, MnO_2 NPs tend to have a linear geometry in the form of O-Mn-O chains, comprising flat zigzag chains in one plane [20].

The use of plant extracts as reducers and surfactants is much more efficient than the chemical method, owing to the presence of various biological molecules in plants [21]. Many effective approaches and methods, including hydrothermal, co-precipitation, sol-gel, and microwave have so far been proposed for the synthesis of MnO_2 NPs [22]. The above-mentioned synthesis methods involve the utilization of chemical surfactants that can have effects on the environment. This can be reduced to some extent by employing green chemistry and plants as surfactants. Green chemistry is a new innovative method that aims to minimize possible harm to humans and the environment. The production of NPs by the green chemistry method together with the use of plants has attracted considerable attention as

a fast, affordable, and biocompatible approach. However, there is no report on the use of cumin extract and Hypericum perforatum plant for the synthesis of MnO_2 NPs and the investigation of their antibacterial and anticancer properties, according to the best of our knowledge.

In this paper, MnO_2 NPs are synthesized by using co-precipitation and green chemistry methods with cumin extract. The resulting NPs are then composited with Hypericum plant. They are also characterized in terms of crystal structure, morphology, and chemical state. Alternatively, antibacterial properties of the MnO_2 NPs in inhibiting Staphylococcus aureus and Pseudomonas aeruginosa bacteria, and their anticancer properties against cervical cancer cells are investigated. These results give insights into the efficient and potential applications of the green synthesized MnO_2 NPs for targeted therapy.

MATERIALS AND METHODS

Co-precipitation and green chemistry methods were used to synthesize MnO_2 NPs. To this end, 0.47 g $KMnO_4$ precursor was dissolved in 20 ml of deionized water. Cumin extract was then added drop by drop to the previous solution and stirred at 40 °C for 2 h using a magnetic stirrer. The resultant solution was dried in an oven at 80 °C. The powder obtained was calcined at 400 °C for 2 h. Finally, the NPs were combined with the Hypericum plant and stirred for 24 h to form the desired nanocomposite.

RESULTS AND DISCUSSION

X-ray diffraction (XRD) pattern

The X-ray diffraction (XRD) pattern of MnO_2 NPs measured in 2θ range of 10°–80° is shown in Fig. 1. Crystal structure of the NPs is found to be α-tetragonal phase, corresponding to the standard card number (044-0141-0141) [23]. No impurity or secondary phase is observed in the pattern. The size of the crystallites was estimated using Scherrer equation (indicating the dependence of particle size on the spread and broadening of diffraction lines) as given below:

$$D = \frac{K\lambda}{\beta \cos\theta} \quad (1)$$

where D is the average size of the crystallites, λ is the wavelength of the X-ray radiation, K is the shape factor (0.9), β is the full width at half maximum (FWHM) of the main peak, and ϑ is the Bragg angle. Accordingly, the average crystallite size of the green synthesized MnO_2 NPs is equal to D= 20 nm.

Scanning and transmission electron microscopy (SEM and TEM) images

To study morphological properties of the MnO_2 NPs, scanning electron microscopy (SEM) and

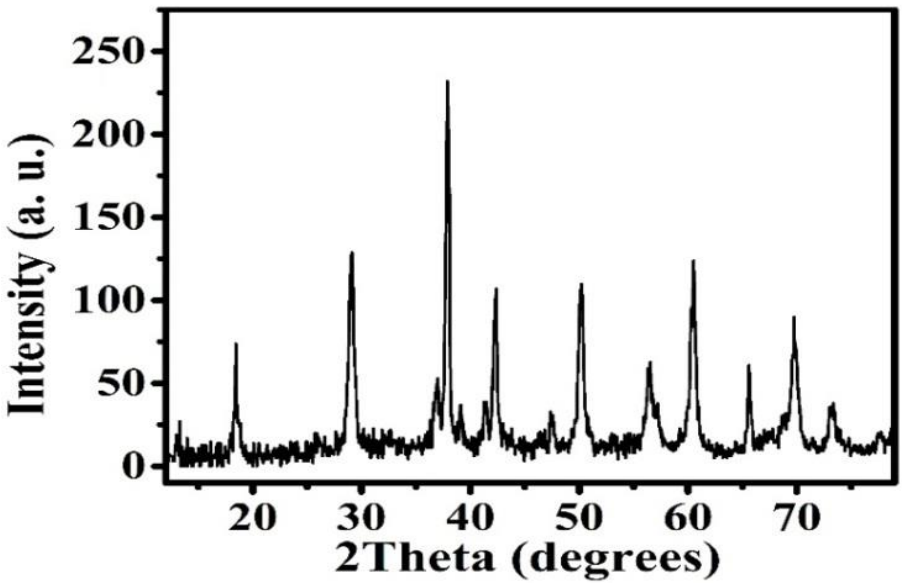

Fig. 1. XRD pattern of MnO_2 NPs synthesized by the co-precipitation and green chemistry methods.

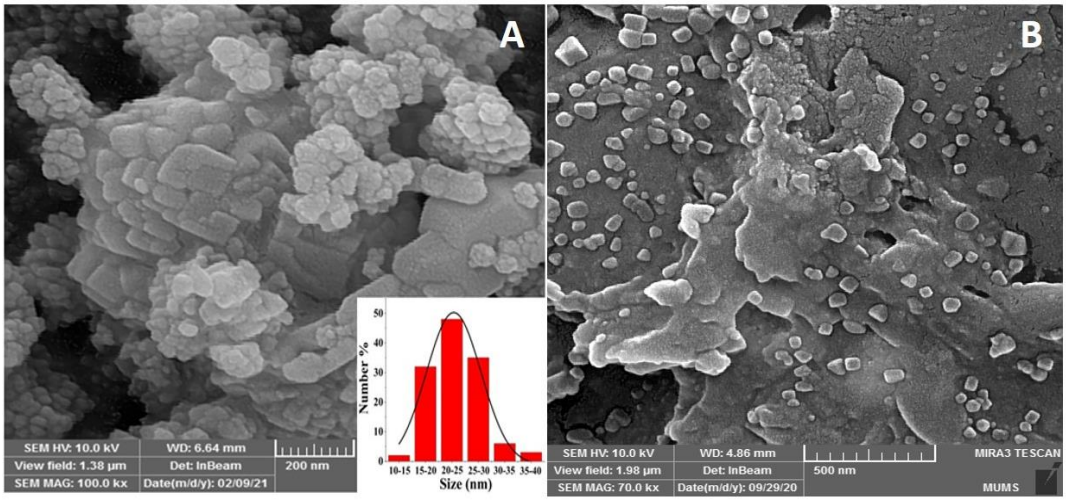

Fig. 2. (A) SEM image of MnO_2 NPs synthesized by co-precipitation and green chemistry methods. The inset shows the corresponding nanoparticle size distribution histogram. (B) SEM image of MnO_2 NPs composited with the Hypericum plant.

transmission electron microscopy (TEM) analyses were carried out, and the results obtained are shown in Figs. 2 and 3, respectively. From Fig. 2(A), SEM image shows that the as-calcined MnO_2 NPs have sizes in the range between 10 and 45 nm (see the inset). The average size of the NPs is found to be approximately 25 nm. It should be noted that the MnO_2 NPs are not homogenous and uniform in all areas due to adhesion and agglomeration. This can be caused by the calcination and exposure to the high temperature, leading to a tendency of the NPs to clump together to reach the minimum energy. Fig. 2(B) shows SEM image of MnO_2 NPs composited with the Hypericum perforatum plant. As can be seen, the resulting composite is less agglomerated than the as-calcined product. In other words, the MnO_2 NPs are spread homogeneously on the surface of the plant, confirming their efficient attachment.

On the other hand, TEM images of the as-calcined and composited MnO_2 NPs are depicted in Fig. 3. The TEM image (Fig. 3(A)) of the as-calcined product reveals that the MnO_2 NPs have spherical-like morphology. The accumulation of some NPs and the enlargement of their dimensions can also be observed. The TEM image (Fig. 3(B)) of the NPs

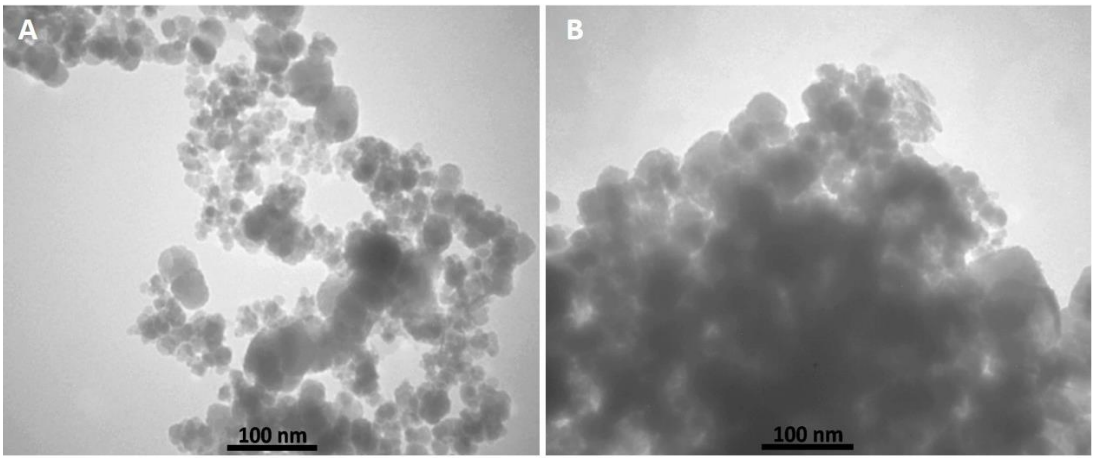

Fig. 3. (A) TEM image of MnO_2 NPs synthesized by co-precipitation and green chemistry methods. (B) TEM image of MnO_2 NPs composited with Hypericum plant.

composited with the Hypericum plant indicates the uniform combination of these two materials, confirming the results obtained from the SEM analysis.

Fourier transform infrared (FTIR) spectra

The formation of ligands and identification of the molecules and functional groups were performed by obtaining Fourier transform infrared (FTIR) spectra of the as-calcined MnO_2 NPs, Hypericum plant, and MnO_2 NPs composited with Hypericum. These results are shown in Fig. 4. From Fig. 4(A), the absorption peaks in the range of 500–600 cm^{-1} are related to Mn-O-Mn vibrations. These peaks are also observed in Fig. 4(C), thereby confirming the binding of the NPs to the plant [24]. The absorption peaks in the 3400–1630 cm^{-1} region are related to the stretching and bending vibrations of H-O bond, which is adsorbed on the surface of the molecule. The 1385 cm^{-1} band is related to bending vibrations of the H-C bond. The absorption peak at 1270 cm^{-1} in the Hypericum plant (Fig. 4(B)) and NPs composited with the plant indicates the presence of C-O aromatic carbon compounds. As well, the existence of CO-O-CO stretching vibrations is observed due to the

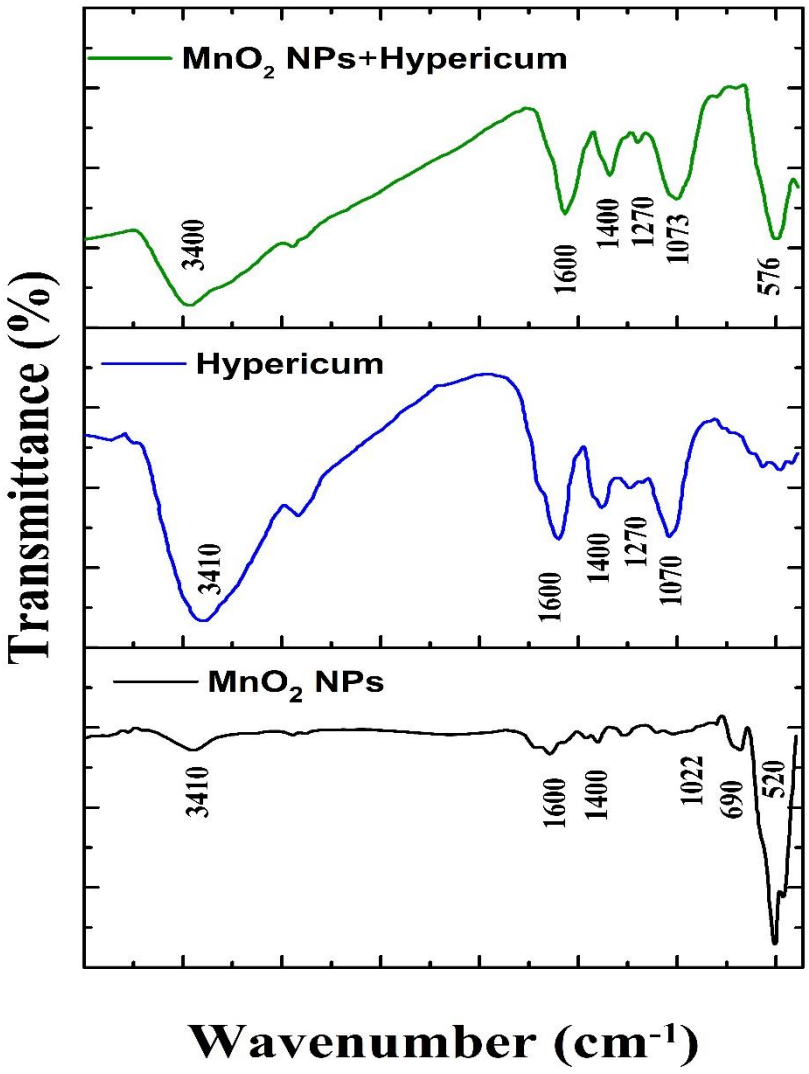

Fig. 4. FTIR spectra of: (A) as-calcined MnO_2 NPs, (B) Hypericum plant, and (C) MnO_2 NPs composited with Hypericum plant.

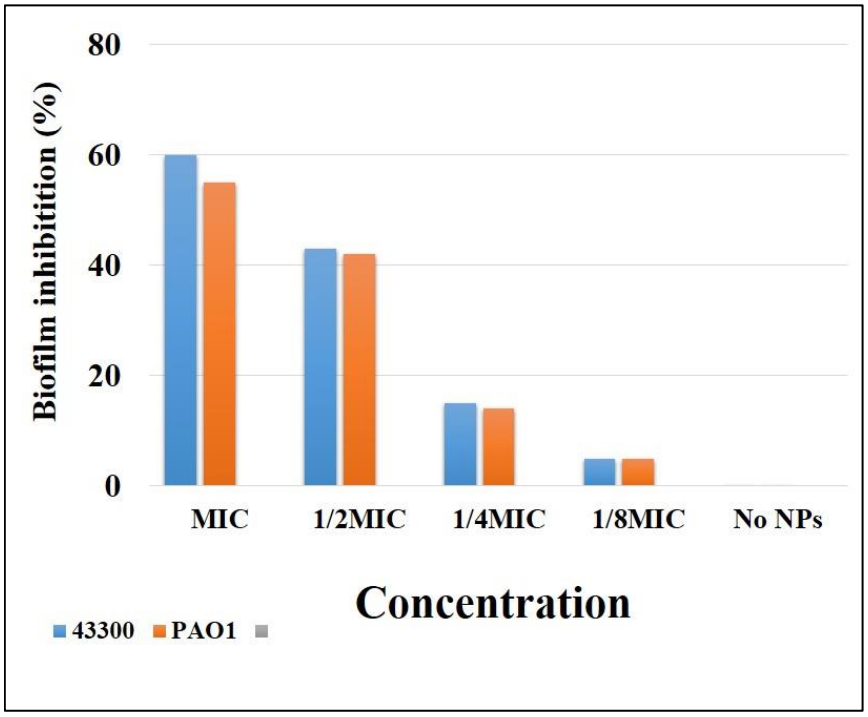

Fig. 5. The effect of different concentrations of MnO_2 NPs composited with Hypericum plant on the reduction of biofilm formation in the standard strains of Staphylococcus aureus ATCC 43300 and Pseudomonas aeruginosa PAO1.

Table 1. Minimum inhibitory concentration (MIC) and minimum bacterial concentration (MBC) of MnO_2 NPs composited with Hypericum plant for Staphylococcus aureus ATCC 43300 and Pseudomonas aeruginosa PAO1.

Microorganism	MnO_2 NPs composited with Hypericum plant			
	MIC		MBC	
	Minimum–Maximum (mg/ml)	Mean ± SD	Minimum–Maximum (mg/ml)	Mean ± SD
S.aureus ATCC 43300	9.50-9.75	9.6±0.13	19.5-39	32.5±11.2
P.aeruginosa PAO1	13.00-13.10	13.50±0.050	27	27

appearance of the peak at 1000 cm^{-1}.

Antimicrobial activity

Antibacterial activity of MnO_2 NPs composited with the Hypericum plant was investigated for Staphylococcus aureus and Pseudomonas aeruginosa strains, and the results obtained are shown in Fig. 5 and Table 1 [25]. Pseudomonas aeruginosa is a gram-negative bacterium that is widespread in all parts of the world and is one of the essential hospital-causing bacteria [26].

Based on the tests performed against the Pseudomonas aeruginosa PAO1 and Staphylococcus aureus ATCC 43300, the resulting minimum–maximum MIC and MBC indicate that the NPs can be used as a medicine to kill bacteria. The effect of different concentrations of NPs on the reduction of biofilm formation in the Staphylococcus aureus ATCC 43300 and Pseudomonas aeruginosa PAO1 standard strains was also studied. Each microplate was used for two bacteria, and a stock of NPs with the same MIC concentration was prepared for each bacterium. The concentration of NPs in the wells was 1/8

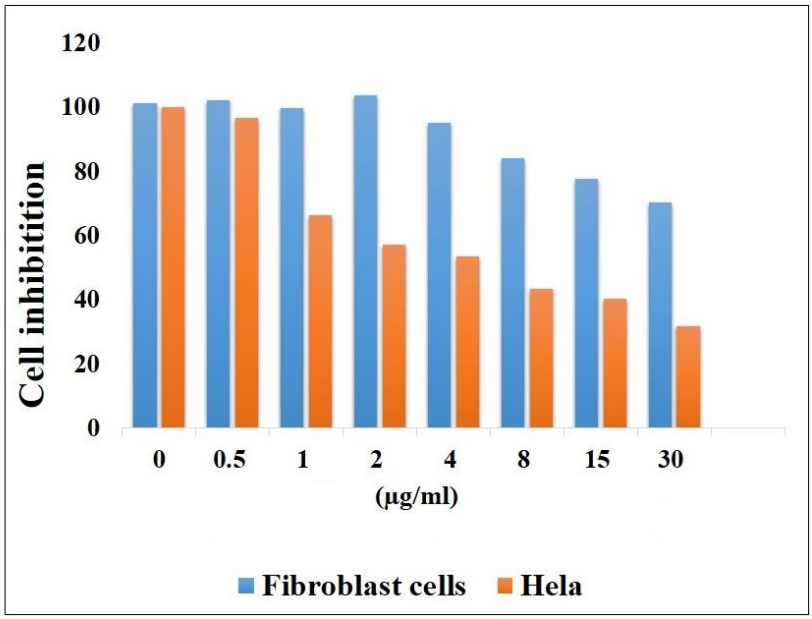

Fig. 6. The toxicity graph of MnO_2 NPs composited with Hypericum plant in Hela and fibroblast cells. The vertical and horizontal axes show the cell viability percentage and different concentrations of the compound treated with the cells, respectively.

MIC, 1/4 MIC, and 1/2 MIC. Moreover, the control was considered with no NPs in one row. As can be seen in Fig. 5, the biofilm formation percentage for the two bacteria decreases significantly with increasing the concentration.

Anticancer properties

In order to evaluate anticancer properties of MnO_2 NPs composited with the Hypericum plant, MTT cytotoxicity test was performed. In this case, the effect of the NPs on the human cervical cancer cell line (Hela) and fibroblast cancer cells was investigated, and the results obtained are shown in Fig. 6. As inferred, the inhibition of Hela and fibroblast cancer cells increases by increasing the concentration of the NPs. Note that the rate of inhibition in Hela cells is higher than that in fibroblast cancer cells. Accordingly, the MnO_2 NPs composited with the Hypericum plant can be selected as a good candidate for the treatment of Hela cancer. In addition, owing to the presence of NPs in the composition, this cancer cell can be treated in a targeted manner.

CONCLUSION

MnO_2 NPs have been initially synthesized by the co-precipitation method using cumin extract, and then composited with Hypericum plant. XRD analysis confirmed the high purity of the NPs with α-tetragonal phase, and the crystallite size of the NPs was estimated to be around 20 nm. The functional groups were investigated and shown by FTIR analysis. Also, the morphology of NPs was investigated by SEM and TEM analyses. The resulting nanocomposite was tested in the laboratory to check its antibacterial and anticancer properties (MTT test), demonstrating good results in inhibiting the formation of biofilms of Staphylococcus aureus and Pseudomonas aeruginosa bacteria. Thus, this nanocomposite can be used in media with the above-mentioned bacteria. Furthermore, MnO_2 NPs composited with the Hypericum plant provided favorable effects on cervical cancer cell inhibition, making them suitable for delivering to the target cancer cell by targeted drug delivery while also preventing the harmful effects of chemotherapy drugs and radiation in radiation therapy on healthy cells.

CONFLICT OF INTEREST

The authors declare that there is no conflict of interests regarding the publication of this

manuscript.

REFERENCES

1. Ansar S, Tabassum H, Aladwan NSM, Naiman Ali M, Almaarik B, AlMahrouqi S, et al. Eco friendly silver nanoparticles synthesis by Brassica oleracea and its antibacterial, anticancer and antioxidant properties. Sci Rep. 2020;10(1).
2. Joshi NC, Siddiqui F, Salman M, Singh A. Antibacterial Activity, Characterizations, and Biological Synthesis of Manganese Oxide Nanoparticles using the Extract of Aloe vera. Asian Pacific Journal of Health Sciences. 2020;7(3):27-29.
3. Liang Z, Wang H, Zhang K, Ma G, Zhu L, Zhou L, et al. Oxygen-defective MnO_2/ZIF-8 nanorods with enhanced antibacterial activity under solar light. Chem Eng J. 2022;428:131349.
4. Mirzaei H. Presence and antimicrobial susceptibility of methicillin-resistant Staphylococcus aureus in raw and pasteurized milk and ice cream in Tabriz by culture and PCR techniques. Afr J Microbiol Res. 2012;6(32).
5. Pier G. Faculty Opinions recommendation of Complete genomes of two clinical Staphylococcus aureus strains: evidence for the rapid evolution of virulence and drug resistance. Faculty Opinions – Post-Publication Peer Review of the Biomedical Literature: Faculty Opinions Ltd; 2004.
6. Ghaznavi-Rad E, Shamsudin MN, Sekawi Z, Khoon LY, Aziz MN, Hamat RA, et al. Predominance and Emergence of Clones of Hospital-Acquired Methicillin-Resistant Staphylococcus aureus in Malaysia. J Clin Microbiol. 2010;48(3):867-872.
7. Pang Z, Raudonis R, Glick BR, Lin T-J, Cheng Z. Antibiotic resistance in Pseudomonas aeruginosa: mechanisms and alternative therapeutic strategies. Biotechnol Adv. 2019;37(1):177-192.
8. Thi MTT, Wibowo D, Rehm BHA. Pseudomonas aeruginosa Biofilms. Int J Mol Sci. 2020;21(22):8671.
9. Bertram JS. The molecular biology of cancer. Mol Aspects Med. 2000;21(6):167-223.
10. Hegde PS, Chen DS. Top 10 Challenges in Cancer Immunotherapy. Immunity. 2020;52(1):17-35.
11. Liu Y, Mi Y, Mueller T, Kreibich S, Williams EG, Van Drogen A, et al. Multi-omic measurements of heterogeneity in HeLa cells across laboratories. Nat Biotechnol. 2019;37(3):314-322.
12. Zhang R, Ji Y, Zhang X, Kennelly EJ, Long C. Ethnopharmacology of Hypericum species in China: A comprehensive review on ethnobotany, phytochemistry and pharmacology. J Ethnopharmacol. 2020;254:112686.
13. Cieplik F, Deng D, Crielaard W, Buchalla W, Hellwig E, Al-Ahmad A, et al. Antimicrobial photodynamic therapy – what we know and what we don't. Crit Rev Microbiol. 2018;44(5):571-589.
14. Abdul-Hamead AA, Othman FM, Fakhri MA. Preparation of MgO–MnO_2 nanocomposite particles for cholesterol sensors. Journal of Materials Science: Materials in Electronics. 2021;32(11):15523-15532.
15. Racik K M, Manikandan A, Mahendiran M, Madhavan J, Victor Antony Raj M, Mohamed MG, et al. Hydrothermal synthesis and characterization studies of α-Fe_2O_3/MnO_2nanocomposites for energy storage supercapacitor application. Ceram Int. 2020;46(5):6222-6233.
16. Yang L, Ren C, Xu M, Song Y, Lu Q, Wang Y, et al. Rod-shape inorganic biomimetic mutual-reinforcing MnO_2-Au nanozymes for catalysis-enhanced hypoxic tumor therapy. Nano Research. 2020;13(8):2246-2258.
17. Das B, Girigoswami A, Pal P, Dhara S. Manganese oxide-carbon quantum dots nano-composites for fluorescence/magnetic resonance (T1) dual mode bioimaging, long term cell tracking, and ROS scavenging. Materials Science and Engineering: C. 2019;102:427-436.
18. Greene A, Hashemi J, Kang Y. Development of MnO₂ hollow nanoparticles for potential drug delivery applications. Nanotechnology. 2020;32(2):025713.
19. Yang G, Ji J, Liu Z. Multifunctional MnO_2 nanoparticles for tumor microenvironment modulation and cancer therapy. WIREs Nanomedicine and Nanobiotechnology. 2021;13(6).
20. Akbari S, Mehdi Foroughi M, Ranjbar M. Solvent-free Synthesis and Characterization of MnO_2 Nanostructures and Investigation of Optical Properties. Journal of Nanomedicine & Nanotechnology. 2018;09(03).
21. Joshi NC, Joshi E, Singh A. Biological Synthesis, Characterisations and Antimicrobial activities of manganese dioxide (MnO_2) nanoparticles. Research Journal of Pharmacy and Technology. 2020;13(1):135.
22. Vella Durai SC, Kumar E, Muthuraj D, Bena Jothy V. Investigation on Electrical and Structural Properties of Manganese Dioxide Nanoparticles. Journal of Nano- and Electronic Physics. 2020;12(3):03011-03011-03011-03015.
23. Kerkar RD, Salker AV. Synergistic effect of modified Pd-based cobalt chromite and manganese oxide system towards NO-CO redox detoxification reaction. Environmental Science and Pollution Research. 2020;27(21):27061-27071.
24. Khalid MU, Warsi MF, Shakir I, Aly Aboud MF, Shahid M, Shar SS, et al. Al^{3+}/Ag^{1+} induced phase transformation of MnO_2 nanoparticles from α to β and their enhanced electrical and photocatalytic properties. Ceram Int. 2020;46(7):9913-9923.
25. Lamers RP, Stinnett JW, Muthukrishnan G, Parkinson CL, Cole AM. Evolutionary Analyses of Staphylococcus aureus Identify Genetic Relationships between Nasal Carriage and Clinical Isolates. PLoS One. 2011;6(1):e16426.
26. Erol S, Altoparlak U, Akcay MN, Celebi F, Parlak M. Changes of microbial flora and wound colonization in burned patients. Burns. 2004;30(4):357-361.